ANALYSIS AND CORRECTION OF SPATIAL DISTORTIONS PRODUCED BY THE GAMMA CAMERA

Steve S. Spector, Valerie A. Brookeman, Chester D. Kylstra, and Nils J. Diaz

University of Florida and Veterans Administration Hospital, Gainesville, Florida

Two types of distortions are produced by the gamma camera. One is nonuniform sensitivity response over the detecting area. The second is spatial distortion; that is, the displacement from their true positions of the x- and y-coordinates of a scintillation. This component of camera image distortion arises in the resolution and transfer of the x- and y-coordinates of a scintillation and results in a nonlinear relationship between the object and the image. The existence of spatial distortions in camera-produced radionuclide images is well known and has been recognized and observed by several workers (*1–6*).

Today because of the present emphasis on computer processing and analysis of the data image, gamma cameras are commonly interfaced to digital computers. This affords an opportunity to quantitatively analyze the inherent distortions introduced by the camera-computer system to any clinical image and to correct them by digital techniques. Nonuniform sensitivity of the camera system may be analyzed by uniformly irradiating the detecting crystal and corrected by storing a digitized matrix of correction factors for subsequent application to any data matrix (*7*). Corrections for sensitivity distortion are applied routinely to digitized images by some laboratories. However, spatial distortions produced by the gamma camera are not currently corrected. The purpose of this study is to determine and evaluate the spatial distortions in radionuclide images caused by a gamma camera and to develop a method for routine correction of these errors by digital computation.

EXPERIMENTAL PROCEDURE

The system investigated is a Pho/Gamma III scintillation camera with conventional S11 phototubes, interfaced to a PDP-8/I digital computer (*8*). Each data image is represented as a 50 × 50 matrix of 2,500 addresses in the computer memory.

The phantom employed for spatial error analysis consists of a 12-in. square Plexiglas base with a grid of 8 × 8 parallel grooves cut at 3-cm intervals in both the x and y directions. The grooves are threaded with plastic tubing of 0.86 mm i.d. and the tubing filled with about 4 mCi of ^{99m}Tc. Technetium-99m is used for the analysis because of its widespread clinical use. The grid source is placed on top of the 4,000-hole technetium collimator with the line sources parallel to the crystal axes. A 20% photopeak window is used for the 140-keV peak, and three million counts are collected in each of five independent studies over a 6-month interval.

The first three studies consider the variations of the spatial distortions introduced by the camera-computer system over a period of time. The grid source has no special positioning on top of the collimator other than that the line sources are parallel to the crystal axes. The last two studies consider the variation of the spatial errors with a 90-deg rotation of the grid source. This tests both the uniformity of the line sources and the reproducibility of the measurements.

All sets of data are corrected for nonuniform sensitivity response of the system by applying correction factors obtained from a ^{99m}Tc crystal flood, collected and stored the same day. A sheet source, placed on top of the collimator, is used for all crystal floods. The correction factor for any data matrix element is inversely proportional to the flood count for that matrix element. The flood-corrected digital data image of the grid is then punched on binary perforated paper tape. Further data processing is performed on an IBM 1800 computing system because of the present limited core memory (8K) of our PDP-8/I.

Received Oct. 26, 1971; original accepted Dec. 2, 1971.

For reprints contact: Valerie A. Brookeman, Dept. of Radiology, University of Florida College of Medicine, Gainesville, Fla. 32601.

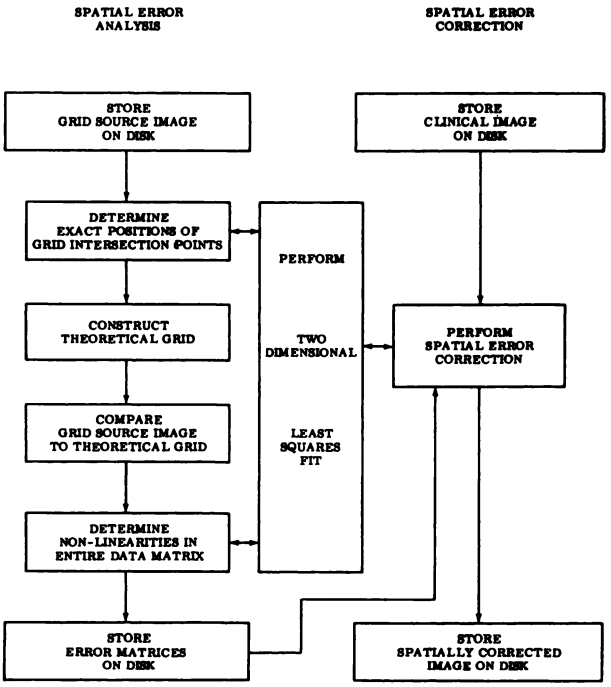

FIG. 1. Flow diagram of spatial error analysis and image correction.

SPATIAL ERROR ANALYSIS

A flow diagram of the computer operations to perform the spatial error analysis and correction is shown in Fig. 1. For spatial error analysis the grid source image is transferred to the disk memory unit of the IBM 1800 computer. The orthogonal grid of 8 × 8 line sources has 64 intersection points, of which about 52 are in the field of view of the camera, as seen in Fig. 2. These 52 intersections of the line sources are identified by the computer and 3 × 3 matrices representing each intersection are stored. The nine data points in each 3 × 3 array are fitted by a least-squares technique to a two-dimensional model, and the position of the maximum value of the model (the peak) is determined. This is used as the exact position of each intersection, as seen by the camera.

If no spatial distortions are introduced by the imaging system, all determined maxima will lie in an exact orthogonal linear array with constant spacing between adjacent maxima. However, the maxima are nonlinearly distributed in the five separate studies. The mean separation (D) between any two adjacent maxima is computed and an ideal theoretical grid constructed with constant line spacing D. The deviations in x and y directions from the theoretical grid are determined for each of the 52 intersection points. The deviations found during the second study are illustrated in Fig. 3. The dotted lines represent the theoretical grid, and the solid lines represent the actual positions of the intersections of the line sources as seen by the camera.

Having determined the x and y deviations of the 52 intersection points from the theoretical grid, the x and y deviations from the theoretical grid are computed for all locations in the data matrix as follows. A two-dimensional asymmetric model is fitted to

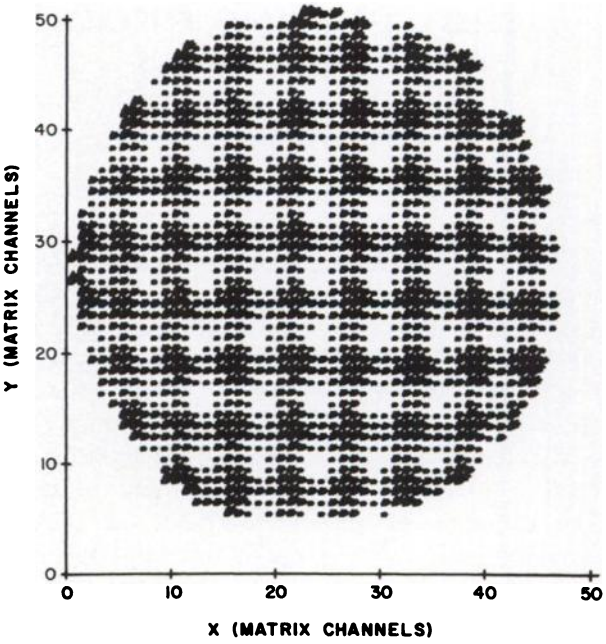

FIG. 2. Image of orthogonal grid of line sources.

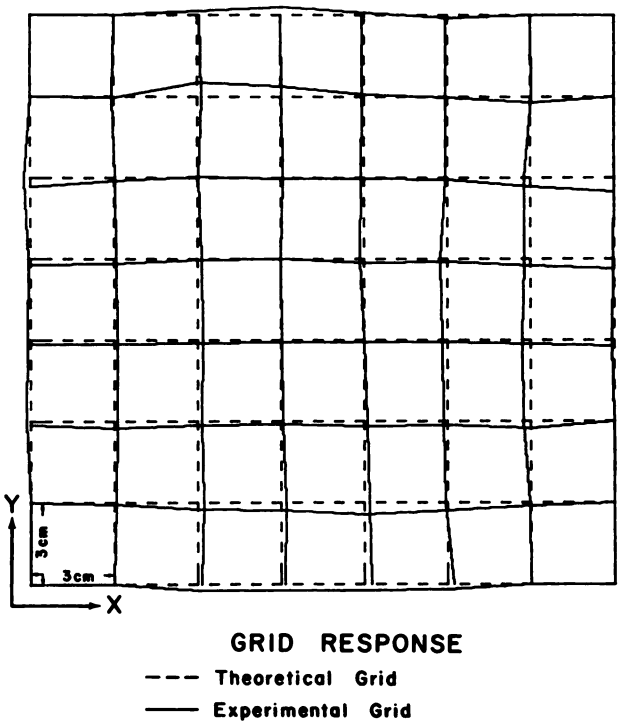

FIG. 3. Line sources as seen by system.

the x deviations of 4 × 4 intersection points by least-squares technique. An x deviation is then determined for every data matrix location in the central square of the 4 × 4 array of intersection points. All x deviations of the 52 intersection points are considered in turn, grouped in 4 × 4 arrays until an x deviation has been determined for every matrix location over the camera face. The deviations in the y direction from the theoretical grid are similarly determined for all data matrix locations. The two resulting error matrices of the x and y nonlinearities, for every point in the data matrix, are stored on disk for future use in correcting the spatial distortions introduced by the gamma camera/PDP-8/I imaging system to radionuclide images.

SPATIAL ERROR CORRECTION

For spatial error correction of any image recorded by the camera-computer system (Fig. 1), the data image is transferred to disk and corrected of spatial distortions by either of two methods, A or B, described below, using the corresponding spatial error arrays. The resulting corrected image is stored on disk and may be displayed in several formats.

Method A shifts each data point in both x and y directions to its correct position, leaving the count content unchanged. This results in nonuniform intervals between adjacent data points and for actual display of an image is impractical due to the grid nature of the output devices. Image correction can also be accomplished by Method B. Here each data point is left in its original, uniform interval position, and a corrected count calculated for each point. This is done by a least-squares technique, taking into account the spatial deviation of each point from its true position. Each data matrix location is considered in turn as the central element in a 3 × 3 array of nine data locations in their true corrected positions. Each 3 × 3 array is fitted into a two-dimensional asymmetric model and a count content for the central element, in its original position, is computed. This is done for each of the data matrix locations over the camera's field of view.

RESULTS

Spatial error analysis of grid. Figure 3 illustrates the grid source as seen by the camera and the computed ideal theoretical grid for the second study as explained above. The x and y deviations of the intersection points from the ideal grid are summarized in Table 1 for the five separate studies performed over a 16-week period. There are no significant differences between the studies.

The deviations from linearity of all data matrix points over the camera face are shown in Fig. 4. The directions of the x and y deviations are given in Fig. 5 for the second and fourth studies. A plus sign indicates a deviation in the positive x or y direction and a minus sign a deviation in the negative x or y direction. The bias of the spatial distortions in both x and y directions are very similar for all studies.

Figure 6 shows the actual magnitudes of the x and y deviations of all points in the data matrix for the second study expressed as the percentage of matrix points with a certain spatial deviation in units of

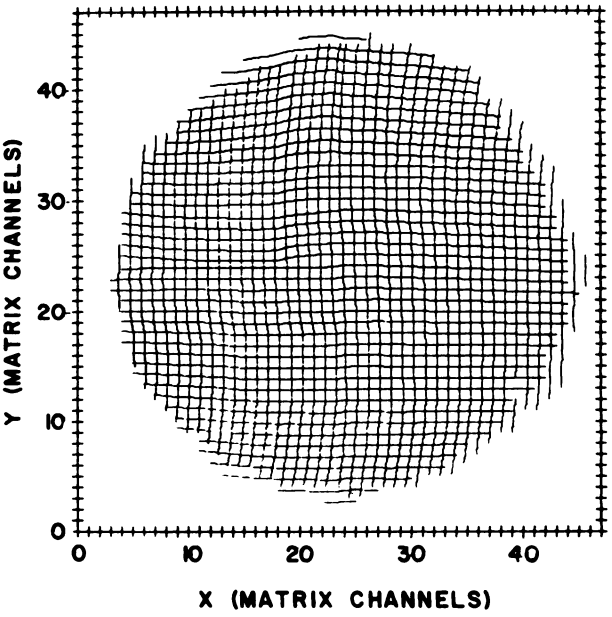

FIG. 4. Data matrix as seen by system.

TABLE 1. DEVIATION FROM LINEARITY OF GRID SOURCE INTERSECTION POINTS

Study No.	X deviation (mm)		Y deviation (mm)	
	Range	Mean (s.d.)	Range	Mean (s.d.)
1	−2.68–+2.95	0.98 (0.79)	−5.54–+5.84	1.70 (1.15)
2	−2.93–+4.15	1.06 (1.13)	−5.17–+1.95	1.37 (0.91)
3	−5.87–+2.17	1.18 (1.03)	−7.18–+2.58	1.16 (0.93)
4	−3.27–+4.68	1.73 (1.51)	−7.76–+2.69	1.53 (1.07)
5	−4.01–+3.56	1.54 (1.22)	−6.60–+4.14	1.40 (0.90)

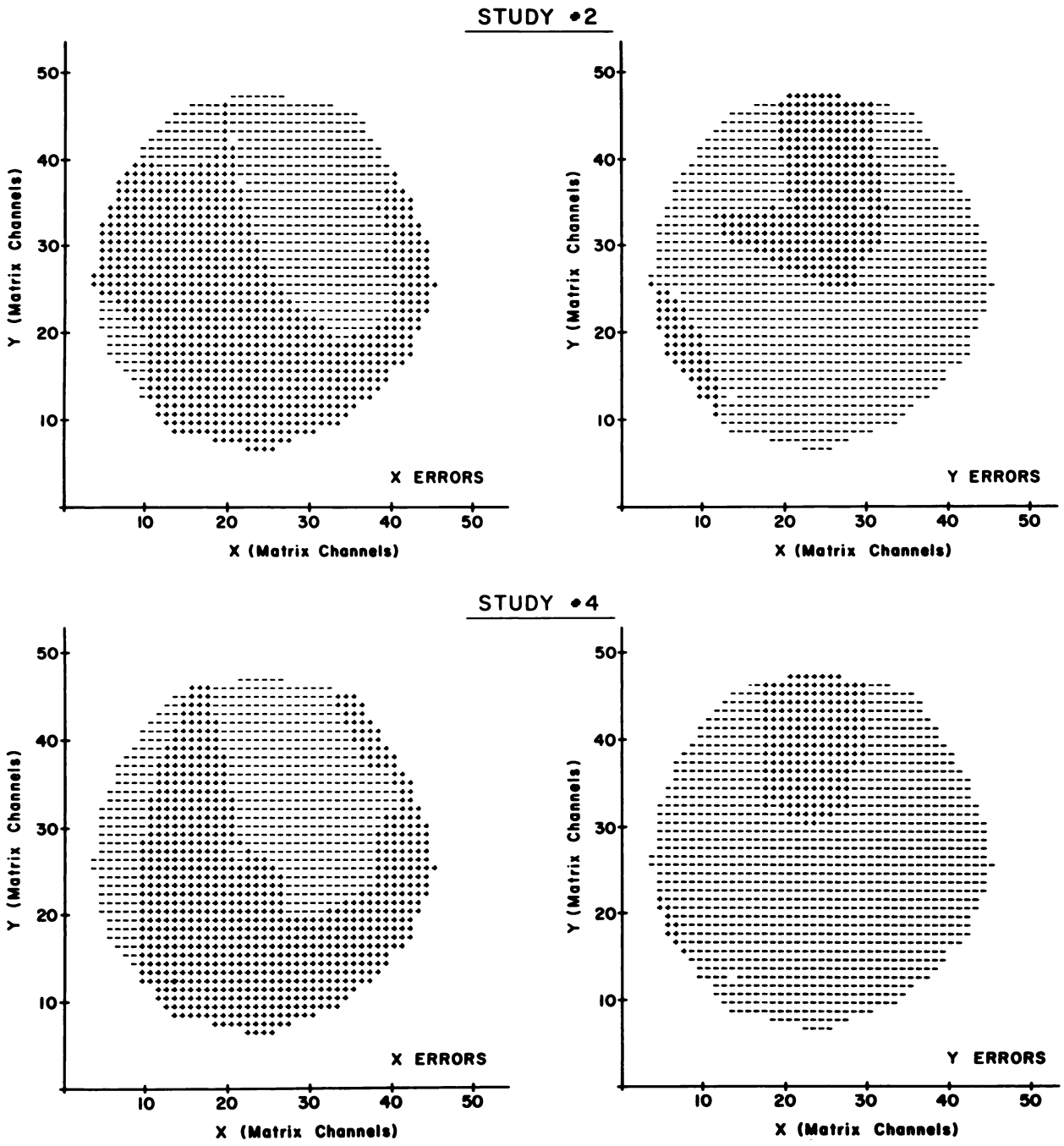

FIG. 5. Bias of deviations from linearity in x and y directions for two independent studies.

matrix channels (1 matrix channel = 6.3 mm). Twenty-five percent of the data matrix points are displaced by more than one half of a channel.

Clinical image correction. Figures 7 and 8 show results of spatial error correction by both Methods A and B for two clinical images. Figure 7 is a cross-sectional count profile through the center of a lung (right lateral view) after injection of 2 mCi of ^{99m}Tc-iron hydroxide aggregates. Figure 8 is a cross-sectional count profile through a right lateral liver after injection of 2 mCi of ^{99m}Tc-sulfur colloid. Half a million counts were collected for each image, and both images were flood-corrected for nonuniform system sensitivity before spatial error correction. Table 2 summarizes the magnitudes of the count changes when the lung image (Fig. 7) is corrected by Method B. Since Method B employs a least-squares fitting technique to calculate a new count for each existing data point as seen by the camera, the image undergoes two-dimensional smoothing in addition to spatial error correction. This is seen in Figs. 7 and 8.

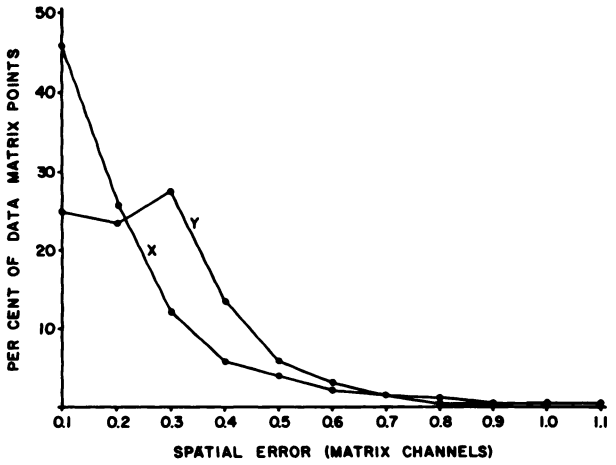

FIG. 6. Distribution of spatial errors in data matrix.

DISCUSSION

Spatial distortions are introduced to radionuclide images by the gamma camera/PDP-8/I computing system. These spatial errors are consistent, both in magnitude and location over the camera face, during at least a 5-month interval. Rotation of the grid source through 90 deg does not change the magnitudes and pattern of the spatial errors indicating independence of source orientation and the "goodness" of the test source.

It is possible to correct any digitized image recorded with the camera-computer system of these spatial distortions by computer techniques. Since the average spatial distortion of any data point is only 0.2 of a matrix channel (about 1.4 mm), it would not appear necessary to routinely correct clinical images for qualitative analysis. However, if a digitized clinical image is to be further processed, for say quantitative analysis, it is essential that corrections be made for spatial errors since the positional error

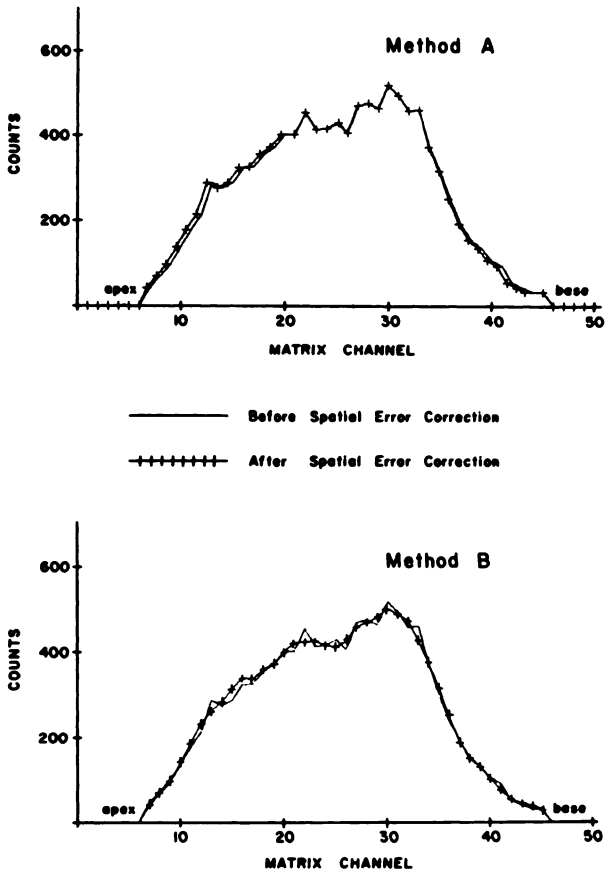

FIG. 7. Cross section through right lateral lung before and after spatial error correction by Methods A and B.

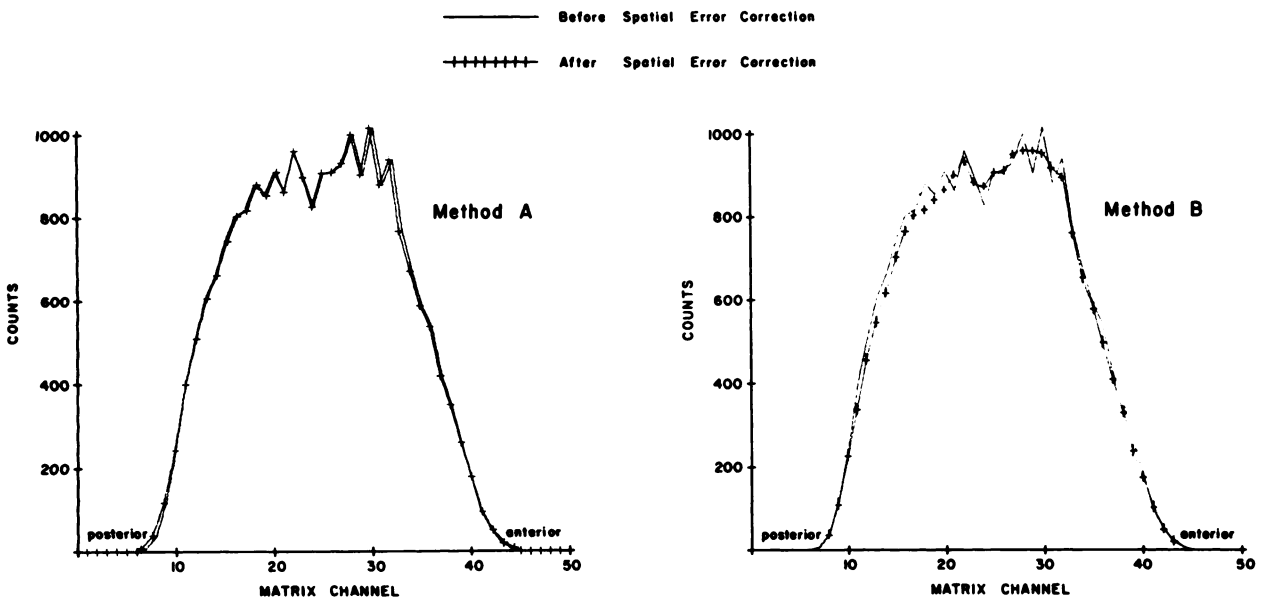

FIG. 8. Cross section through right lateral liver before and after spatial error correction by Methods A and B.

TABLE 2. COUNT CHANGES IN RIGHT LATERAL LUNG IMAGE AFTER SPATIAL ERROR CORRECTION BY METHOD B

Percentage data matrix points	Count change (s.d.)
76	≤1
20	1–2
3	2–3
1	3–4

of any one data point may be as high as 1.1 of a matrix channel (7 mm).

SUMMARY

Spatial distortions introduced to radionuclide images from a gamma camera/PDP-8/I computing system have been investigated by analyzing the response of the system using a 4,000-hole technetium collimator to a defined orthogonal grid source of ^{99m}Tc. The 50 × 50 data matrix of the grid image was first corrected for nonuniform sensitivity response, and the nonlinearities in the image were analyzed using programs developed for an IBM 1800 computing system. Spatial distortions ranged from −7.8 to 5.8 mm with 30% of the data matrix points distorted more than 3.2 mm. Spatial errors were consistent, both in magnitude and location, over the camera face during a 5-month period.

A software routine has been developed for the IBM 1800 which either shifts each data point in any radionuclide image to its correct location, leaving the count content unchanged, or, leaving each data point in its original position, calculates the correct number of counts for the location in question. The latter alternative maintains the uniform intervals between the digitized data points and hence is more convenient for display of clinical data by an output device. These techniques may be applied to any digitized clinical image to correct for spatial distortions.

REFERENCES

1. MALLARD JR, MYERS MJ: The performance of a gamma camera for the visualization of radioactive isotopes in vivo. *Phys Med Biol* 8: 165–182, 1963

2. CRADDUCK TD, FEDORUK SO, REID WB: A new method of assessing the performance of scintillation cameras and scanners. *Phys Med Biol* 11: 423–435, 1966

3. MYERS MJ, KENNY PJ, LAUGHLIN JS: Quantitative analysis of data from scintillation cameras. *Nucleonics* 24: No 2, 58–61, 1966

4. ANGER HO: Radioisotope cameras. In *Instrumentation in Nuclear Medicine,* vol 1, New York, Academic Press, 1967, p 511

5. JAHNS E, HINE GJ: A line-source phantom for testing the performance of scintillation cameras. *J Nucl Med* 8: 829–836, 1967

6. SVEDBERG JB: Image quality of a gamma camera system. *Phys Med Biol* 13: 597–610, 1968

7. MORRISON LM, BRUNO FP, MAUDERLI W: Sources of gamma-camera image inequalities. *J Nucl Med* 12: 785–791, 1971

8. BRUNO FP, BROOKEMAN VA, WILLIAMS CM: A digital computer data acquisition, display and analysis system for the gamma camera. *Radiology* 96: 658–661, 1970